Pramana – J. Phys. (2022) 96:33
https://doi.org/10.1007/s12043-021-02277-9

Teleporting DV qubit to CV qubit and vice versa via DV-CV hybrid entanglement across lossy environment supervised simultaneously by both DV and CV controllers

CAO THI BICH[1,2,*] and NGUYEN BA AN[2,3]

[1]Graduate University of Science and Technology, Vietnam Academy of Science and Technology, 18 Hoang Quoc Viet, Cau Giay, Hanoi, Vietnam
[2]Center for Theoretical Physics, Institute of Physics, Vietnam Academy of Science and Technology (VAST), 18 Hoang Quoc Viet, Cau Giay, Hanoi, Vietnam
[3]Thang Long Institute of Mathematics and Applied Sciences (TIMAS), Thang Long University, Nghiem Xuan Yem, Hoang Mai, Hanoi, Vietnam
*Corresponding author. E-mail: caobichvatly@gmail.com

MS received 13 August 2021; revised 21 September 2021; accepted 28 September 2021

Abstract. A salient merit of processing quantum information is the ability of simultaneously working with both bit zero and bit one. The basic unit of quantum information, the so-called qubit, is a superposition of two orthogonal (or near-orthogonal) quantum states which can be realised on distinct physical platforms. At present, no unique qubit encoding exists that is superior to all the other ones. Different labs are implementing their most convenient technique for encoding the qubit and so the network of labs becomes heterogeneous. In this paper, we consider two types of qubit encodings, one is the single-rail qubit in terms of discrete-variable (DV) states $|0\rangle$ and $|1\rangle$ which are respectively the vacuum and the single-photon state and the other is the coherent-state qubit in terms of continuous-variable (CV) states $|\alpha\rangle$ and $|-\alpha\rangle$ which are coherent states with equal amplitudes but opposite phases. We devise linear-optics schemes to teleport one type of qubit to the other type. More than that, our teleportation schemes are designed so that two kinds of controllers, one is capable of manipulating single-rail qubits (DV controller) while the other coherent-state ones (CV controller), are able to simultaneously supervise the tasks in both directions. We first propose a quantum circuit to prepare a relevant four-party pure entangled state serving as a quantum channel between the four participants: two teleporters and two controllers. We then detail the hybrid controlled teleportation protocols taking into account the dissipation effect caused by the presence of losses in the environment surrounding the participants.

Keywords. Controlled teleportations; lossy environment; single-rail qubit encoding; coherent-state qubit encoding.

PACS Nos **03.67.-a; 03.65.Ud; 03.67.Hk**

1. Introduction

Quantum information encoded in quantum states provides a totally novel way of information processing that enables one to execute intriguing tasks which would not be possible by means of traditional classical methods [1]. Information can be encoded either in particle-like discrete-variable (DV) states [2,3], which live in finite-dimensional Hilbert spaces, or in wave-like continuous-variable (CV) states [4–6], whose Hilbert spaces are of infinite dimension. DV approach, which relies mainly on using single photons, entangled photon pairs, passive linear-optics devices and photodetectors, can achieve close-to-unity fidelity. However, the Bell-state measurement, which is the prerequisite for many quantum protocols, cannot be performed deterministically by means of linear optics and photodetections because only two of the four Bell states can be identified with certainty [7]. Thus, the DV teleportation success probability could not exceed $1/2$ [8,9]. On the other hand, CV approach, which acts on macroscopic continuous-variable states and their superpositions, has some prominent benefits

Published online: 25 January 2022

such as unconditional operations, high detection efficiencies and the Bell-state measurement for entangled coherent states can be performed in a near-deterministic manner [10,11]. However, the CV teleportation fidelity is modest because the CV entanglement degree is usually limited. Since both DV and CV encodings have their own advantages and drawbacks [1,7–9,12–14], combining these two approaches to form the so-called hybrid approach has become topical in quantum communication and quantum computation. Such a hybrid approach might provide positive features of each approach while at the same time overcomes their intrinsic negative effects [15,16]. It also promises potential applications by encoding information exploiting the wave–particle degrees of freedom [17–23]. Recently, generation and manipulation of hybrid entangled states have not only attracted much attention in theory but also obtained several significant demonstrations in experiment [24–26]. It appeared as essential resources for some important tasks within a heterogeneous quantum network [23,27–29], generation of non-Gaussian states [30], hybrid teleportation [15,31] and so on. For examples, Ralph *et al* discussed a scheme to perform teleportation between a dual-rail qubit (superposition of two orthogonally polarised states of a photon) and a single-rail qubit (superposition of vacuum and single-photon states) [32]. Park *et al* [31] and Jeong *et al* [33] studied quantum teleportation between a polarised single-photon qubit and a coherent-state qubit as well as between a single-rail qubit and a coherent-state qubit using hybrid entanglement between those two types of qubits, respectively. To address practical conditions for such quantum information transfers, it would be important to take into account decoherence effects caused by photon losses that are typical in optical systems embedded in dissipative environments. Also, in practice it often appears necessary to quantumly control a global task. This can be realised by adding controllers who are also entangled with the other authorised parties and have the right at the last minute to decide completion of a task after carefully considering all the concerned situations, including non-technical issues.

The tasks of our concern in this work are hybrid controlled teleportations between two particular types of qubits: single-rail qubit and coherent-state qubit. Concretely, let Alice, Bob, Charlie and David be four parties who are far apart from each other and allowed to perform only local operations and classical communication. Alice and Charlie are DV parties who are able to work only with single-rail qubits while Bob and David are CV parties who are only capable of manipulating coherent state qubits. Our purpose is to devise protocols that allow teleportations in both directions, from a single-rail qubit to a coherent-state qubit as well as from a coherent-state qubit to a single-rail qubit, across a lossy environment under simultaneous control of both DV Charlie and CV David. The formulation of our tasks and a scheme to generate the relevant working quantum channel are presented in §2. In §3 the affect of dissipation caused by the lossy environment on the quantum channel is investigated. Section 4 details the hybrid controlled teleportations using the dissipated quantum channel. Comparisons of the average fidelities and success probabilities between teleportations in opposite directions are given in §5. Section 6 concludes and raises some possible problems to be studied in future.

2. Formulation of the tasks and their relevant quantum channel

As mentioned already, we are interested in teleporting a DV qubit to a CV qubit and vice versa. We shall consider these tasks separately. The first task is that Alice holds a single-rail qubit in state

$$|\psi_{\rm DV}\rangle = a\,|0\rangle + b\,|1\rangle, \tag{1}$$

where $|0\rangle$ ($|1\rangle$) is the vacuum (the single-photon) state and a, b are unknown complex coefficients satisfying the normalisation constraint $|a|^2 + |b|^2 = 1$. She needs to securely transfer to Bob the coefficients a, b in terms of a coherent-state qubit state

$$|\psi_{\rm CV}(\alpha)\rangle = N(a\,|\alpha\rangle + b\,|-\alpha\rangle), \tag{2}$$

where $|\pm\alpha\rangle$ are coherent states with complex amplitudes $\pm\alpha$ and $N = N(a, b, \alpha) = (1 + 2Re(a^*b)e^{-2|\alpha|^2})^{-1/2}$ is to normalise the state $|\psi_{\rm CV}(\alpha)\rangle$. The second task, inverse to the first one, is that Bob holds an unknown coherent-state qubit in state (2) and needs to securely transfer to Alice the coefficients a, b in terms of a single-rail qubit state (1). We aim at designing protocols such that both the tasks are simultaneously supervised by two controllers Charlie and David, with Charlie being able to work only with DV single-rail states while David being only capable of manipulating CV coherent-state qubits. Each of the two tasks could only be completed upon permission of both the controllers.

To execute either of the two tasks by means of local operations and classical communication, the four parties Alice, Bob, Charlie and David should share in advance a relevant hybrid DV–CV four-party quantum entanglement in terms of the pure entangled state of the form

$$|\Gamma(\alpha)\rangle_{1234} = \frac{1}{\sqrt{2}}(|\alpha, \alpha, 0, 0\rangle + |-\alpha, -\alpha, 1, 1\rangle)_{1234}, \tag{3}$$

where $|\alpha, \alpha, 0, 0\rangle_{1234}$ and $|-\alpha, -\alpha, 1, 1\rangle_{1234}$ are short for $|\alpha\rangle_1 \otimes |\alpha\rangle_2 \otimes |0\rangle_3 \otimes |0\rangle_4$ and $|-\alpha\rangle_1 \otimes |-\alpha\rangle_2 \otimes |1\rangle_3 \otimes$

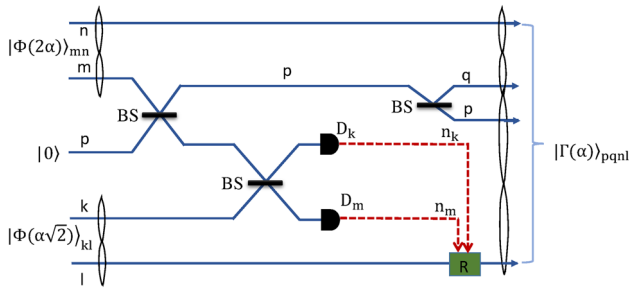

Figure 1. Quantum circuit to produce the hybrid entanglement defined by eq. (3). BS denotes a beam-splitter, which acts on two modes as $\mathrm{BS}_{xy}(\pi/4) = \exp[\pi(a_x^+ a_y - a_y^+ a_x)/4]$. The solid line labelled n (k, l, m, n, p and q) represents mode n (k, l, m, n, p and q). D_k and D_m are photodetectors to count the photon numbers in the corresponding modes. The dashed lines represent the numbers n_k and n_m of the detected photons. $R = I, X, Z$ or XZ conditioned on the detected numbers of photons.

$|1\rangle_4$, respectively. In order to prepare the pure hybrid entangled state (3), we need the following initial state:

$$|\Psi_0(\alpha)\rangle_{klmn} = \left|\Phi(\alpha\sqrt{2})\right\rangle_{kl} |\Phi(2\alpha)\rangle_{mn}\,, \tag{4}$$

where

$$|\Phi(\gamma)\rangle_{xy} = \frac{1}{\sqrt{2}}(|\gamma, 0\rangle + |-\gamma, 1\rangle)_{xy} \tag{5}$$

is a hybrid entangled state between a coherent state and a single-rail state which can be produced using the photon addition techniques [25]. Supplied with the state (4), our three-step scheme for the preparation of state (3) is sketched in figure 1.

Step 1. Mode m of the state $|\Phi(2\alpha)\rangle_{mn}$ is sent to a beam-splitter denoted by BS, which acts on two modes x, y as $\mathrm{BS}_{xy}(\pi/4) = \exp[\pi(a_x^+ a_y - a_y^+ a_x)/4]$, with $a_j^+(a_j)$ the photon creation (annihilation) operator of mode j. Action of such a combined device on $|\Psi_0\rangle_{klmn}$ transforms it to

$$|\Psi_1\rangle_{klmnp} = \mathrm{BS}_{mp}\,|\Psi_0\rangle_{klmn}\,, \tag{6}$$

with p a new mode emerging as the reflected mode after the first BS (see figure 1).

Step 2. Mode m, which has just passed through the first BS, is mixed with mode k of the state $|\Phi(\alpha\sqrt{2})\rangle_{kl}$ on another BS. As a result, $|\Psi_1\rangle_{klmnp}$ becomes

$$|\Psi_2\rangle_{klmnp} = \mathrm{BS}_{mk}\,|\Psi_1\rangle_{klmnp}\,. \tag{7}$$

Behind the device BS_{mk} (which is the second BS in figure 1) two photodetectors, D_m and D_k, are placed to count the photon number n_m and n_k of the outgoing modes m and k, respectively. The state of modes l, n and p are projected onto

$$|\Psi_3\rangle_{lnp} = \frac{{}_{mk}\langle n_m, n_k\,|\Psi_2\rangle_{klmnp}}{\sqrt{P_{n_m n_k}}}, \tag{8}$$

with

$$P_{n_m n_k} = |{}_{mk}\langle n_m, n_k\,|\Psi_2\rangle_{klmnp}\,|^2 \tag{9}$$

the corresponding probability. Five possibilities are labelled from (i) to (v) as follows:

(i) If $n_m =$ even $\neq 0$ and $n_k = 0$, then the state $|\Psi_3\rangle_{pnl}$ in eq. (8) is

$$|\Psi_3^{(i)}\rangle_{pnl} = \frac{1}{\sqrt{2}}(|\alpha\sqrt{2}, 0, 0\rangle + |-\alpha\sqrt{2}, 1, 1\rangle)_{pnl}, \tag{10}$$

which happens with a probability

$$P_{\mathrm{even}\neq 0,0} = \frac{1}{2}\mathrm{e}^{-4|\alpha|^2}[\cosh(4|\alpha|^2) - 1]. \tag{11}$$

(ii) If $n_m =$ odd and $n_k = 0$, then the state $|\Psi_3\rangle_{lnp}$ in eq. (8) is

$$|\Psi_3^{(\mathrm{ii})}\rangle_{pnl} = \frac{1}{\sqrt{2}}(|\alpha\sqrt{2}, 0, 0\rangle - |-\alpha\sqrt{2}, 1, 1\rangle)_{pnl}, \tag{12}$$

which happens with a probability

$$P_{\mathrm{odd},0} = \frac{1}{2}\mathrm{e}^{-4|\alpha|^2}\sinh(4|\alpha|^2). \tag{13}$$

(iii) If $n_m = 0$ and $n_k =$ even $\neq 0$, then the state $|\Psi_3\rangle_{pnl}$ in eq. (8) is

$$|\Psi_3^{(\mathrm{iii})}\rangle_{pnl} = \frac{1}{\sqrt{2}}(|\alpha\sqrt{2}, 0, 1\rangle + |-\alpha\sqrt{2}, 1, 0\rangle)_{pnl}, \tag{14}$$

which happens with a probability $P_{0,\mathrm{even}\neq 0} = P_{\mathrm{even}\neq 0,0}$.
(iv) If $n_m = 0$ and $n_k =$ odd, then the state $|\Psi_3\rangle_{pnl}$ in eq. (8) is

$$|\Psi_3^{(\mathrm{iv})}\rangle_{pnlq} = \frac{1}{\sqrt{2}}(|\alpha\sqrt{2}, 0, 1\rangle - |-\alpha\sqrt{2}, 1, 0\rangle)_{pnl}, \tag{15}$$

which happens with a probability $P_{0,\mathrm{odd}} = P_{\mathrm{odd},0}$.
(v) If $n_m = n_k = 0$, then the state $|\Psi_3\rangle_{pnl}$ in eq. (8) is

$$|\Psi_3^{(v)}\rangle_{pnl} = \frac{1}{2}(|\alpha\sqrt{2}, 0, 0\rangle + |\alpha\sqrt{2}, 0, 1\rangle + |-\alpha\sqrt{2}, 1, 0\rangle + |-\alpha\sqrt{2}, 1, 1\rangle)_{pnl}, \tag{16}$$

which happens with a probability $P_{00} = \mathrm{e}^{-4|\alpha|^2}$.

Step 3. Now, input mode p, which is the mode reflected from the first BS, to a third BS after which a new

reflected mode appears which is labelled by q. Thus, the states (10)–(16) respectively become

$$|\Psi_4^{(i)}\rangle_{pqnl} = \frac{1}{\sqrt{2}}(|\alpha, \alpha, 0, 0\rangle + |-\alpha, -\alpha, 1, 1\rangle)_{pqnl}, \tag{17}$$

$$|\Psi_4^{(ii)}\rangle_{pqnl} = \frac{1}{\sqrt{2}}(|\alpha, \alpha, 0, 0\rangle - |-\alpha, -\alpha, 1, 1\rangle)_{pqnl}, \tag{18}$$

$$|\Psi_4^{(iii)}\rangle_{pqnl} = \frac{1}{\sqrt{2}}(|\alpha, \alpha, 0, 1\rangle + |-\alpha, -\alpha, 1, 0\rangle)_{pqnl}, \tag{19}$$

$$|\Psi_4^{(iv)}\rangle_{pqnl} = \frac{1}{\sqrt{2}}(|\alpha, \alpha, 0, 1\rangle - |-\alpha, -\alpha, 1, 0\rangle)_{pqnl} \tag{20}$$

and

$$|\Psi_4^{(v)}\rangle_{pqnl} = \frac{1}{2}(|\alpha, \alpha, 0\rangle + |-\alpha, -\alpha, 1\rangle)_{pqn}(|0\rangle + |1\rangle)_l. \tag{21}$$

We see that $|\Psi_4^{(v)}\rangle_{pqnl}$ cannot be unitarily transformed to $|\Gamma(\alpha)\rangle_{pqnl}$, while

$$|\Psi_4^{(i)}\rangle_{pqnl} = |\Gamma(\alpha)\rangle_{pqnl},$$

$$|\Psi_4^{(ii)}\rangle_{pqnl} = Z_l\,|\Gamma(\alpha)\rangle_{pqnl},$$

$$|\Psi_4^{(iii)}\rangle_{pqnl} = X_l\,|\Gamma(\alpha)\rangle_{pqnl}$$

and

$$|\Psi_4^{(iv)}\rangle_{pqnl} = -Z_l X_l\,|\Gamma(\alpha)\rangle_{pqnl}.$$

Z_l stands for the transformation $\{|0\rangle_l \to |0\rangle_l, |1\rangle_l \to -|1\rangle_l\}$ which can easily be implemented deterministically by a π-phase-shifter $P_l(\pi)$. X_l stands for the transformation $\{|0\rangle_l \to |1\rangle_l, |1\rangle_l \to |0\rangle_l\}$ which cannot directly be done on a single-rail qubit, but can indirectly with a probability of 1/2 with the assistance of additional resources and operations. Therefore, the total probability P_Γ for the successful preparation of the quantum channel $|\Gamma\rangle$ in eq. (3) is

$$P_\Gamma = \frac{3}{2}(P_{\text{even}\neq 0,0} + P_{\text{odd},0}) = \frac{3}{4}(1 - \mathrm{e}^{-4|\alpha|^2}), \tag{22}$$

which saturates to 75% for $|\alpha| \geq 1.3$. However, the probabilistic feature of the hybrid entanglement preparation scheme is not an issue because the state preparation process is regarded as an off-line procedure.

3. Influence of lossy environment on the quantum channel

The prepared hybrid pure entangled state $|\Psi_4^{(i)}\rangle_{pqnl}$ in eq. (17) is exactly the desired state $|\Gamma(\alpha)\rangle_{pqnl}$ defined by eq. (3) which serves as the working quantum channel to be shared among the four authorised parties to carry out the two tasks specified in the previous section. For convenience, we change the modal labels as $p \to 1$, $q \to 2$, $n \to 3$ and $l \to 4$, i.e., $|\Gamma(\alpha)\rangle_{pqnl} \to |\Gamma(\alpha)\rangle_{1234}$. The modes of such a quantum channel must be distributed so that Alice receives mode 4, David mode 2, Charlie mode 3 and Bob mode 1. During the modes' distribution, photon losses occur due to interaction with the surrounding lossy environment or, in other words, the quantum channel suffers from dissipation. The dissipation effect can be described, within the framework of the Born–Markov approximation at zero temperature, by the master equation [34]

$$\frac{\partial \rho_{1234}(t)}{\partial t} = (J + L)\rho_{1234}(t), \tag{23}$$

where t is the time of optical environment interaction, $\rho_{1234}(t)$ is the density matrix of the quantum channel at time t, while J and L are the Lindblad superoperators acting on $\rho_{1234}(t)$ as

$$J\rho_{1234}(t) = \gamma \sum_i a_i \rho_{1234}(t) a_i^+$$

and

$$L\rho_{1234}(t) = -\frac{\gamma}{2}\sum_i (a_i^+ a_i \rho_{1234}(t) + \rho_{1234}(t) a_i^+ a_i),$$

where γ is the decay constant determined by the strength of quantum channel–environment interaction and a_i (a_i^+) is the annihilation (creation) operator of mode i. The formal solution of eq. (23) can be represented as

$$\rho_{1234}(t) = \exp[(J + L)t]\rho_{1234}(0), \tag{24}$$

where $\rho_{1234}(t = 0) = |\Gamma\rangle_{1234}\langle\Gamma|$ is the initial pure state of the quantum channel. Using the above action rules of J and L we obtain the dissipated density matrix $\rho_{1234}(\tau)$ as follows:

$$\begin{aligned}\rho_{1234}(\tau) = \frac{1}{2}\{&[|\tau\alpha\rangle_1\langle\tau\alpha| \otimes |\tau\alpha\rangle_2\langle\tau\alpha| \\ &\otimes|0\rangle_3\langle 0| \otimes |0\rangle_4\langle 0| \\ &+C\tau^2|\tau\alpha\rangle_1\langle-\tau\alpha| \otimes |\tau\alpha\rangle_2\langle-\tau\alpha| \\ &\otimes|0\rangle_3\langle 1| \otimes |0\rangle_4\langle 1| \\ &+C\tau^2|-\tau\alpha\rangle_1\langle\tau\alpha| \otimes |-\tau\alpha\rangle_2\langle\tau\alpha| \\ &\otimes|1\rangle_3\langle 0| \otimes |1\rangle_4\langle 0| \\ &+|-\tau\alpha\rangle_1\langle-\tau\alpha| \otimes |-\tau\alpha\rangle_2\langle-\tau\alpha|\end{aligned}$$

$$\otimes(\tau^2 |1\rangle_3 \langle 1| + (1-\tau^2) |0\rangle_3 \langle 0|)$$
$$\otimes(\tau^2 |1\rangle_4 \langle 1| + (1-\tau^2) |0\rangle_4 \langle 0|)\}, \quad (25)$$

where $C = \mathrm{e}^{-4(1-\tau^2)\alpha^2}$ and $\tau = \mathrm{e}^{-\gamma t/2}$. Note that $\tau = 1$ when $\gamma t = 0$ (i.e., when $\gamma = 0$ or/and $t = 0$), while $\tau \to 0$ when $\gamma t \to \infty$ (e.g., when γ is finite but $t \to \infty$). That is, for a fixed γ, τ is varying from 1 to 0 as time is evolving from $t = 0$ to $t = \infty$. So, as inspected from eq. (25), the dissipation reduces amplitudes of the coherent-state modes 1 and 2 from $\pm\alpha$ to $\pm\tau\alpha$ and, at the same time, transits the one-photon state $|1\rangle \langle 1|$ of the single-rail modes 3 and 4 into the zero-photon one $|0\rangle \langle 0|$ (note that such a photon loss of the single-rail qubits does not kick the qubits out off their qubit spaces and can be looked upon as a bit-flip error that could be corrected by a quantum error-correction code). In the following, to account for the dissipation effect, we shall use as the state of the working quantum channel the mixed state $\rho_{1234}(\tau)$, eq. (25), rather than the pure one $|\Gamma\rangle_{1234}$, eq. (3).

4. Hybrid-controlled teleportations

Here, by hybrid-controlled teleportations we mean the remote transfer, by means of local operations and classical communication, of an unknown quantum information encoded in DV states at Alice's station to the quantum information encoded in CV states at Bob's station and vice versa, in such a way that the teleportation either in the Alice-to-Bob direction or in the Bob-to-Alice one is supervised by a number of DV and CV controllers. In this work, we consider two controllers: one (Charlie) is working with DV states while the other (David) with CV ones. As for the DV participants (Alice and Charlie), we assume that they work with the so-called single-rail logic, i.e., the qubit is a superposition of the zero-photon state $|0\rangle$, representing the logical value zero, and the one-photon state $|1\rangle$, representing the logical value one. Contrary to Alice and Charlie, Bob and David (the CV participants) are assumed to work with the encoding such that the qubit is a superposition of two coherent states $|\pm\alpha\rangle$ of which $|-\alpha\rangle$ represents the logical value zero and $|\alpha\rangle$ represents the logical value one.

4.1 *Controlled teleportation from a single-rail qubit to a coherent-state qubit*

This is the first task mentioned in §2. Suppose that Alice has a single-rail qubit A in an unknown state $|\psi_{\mathrm{DV}}\rangle_A = (a|0\rangle + b|1\rangle)_A$ and she needs to teleport $|\psi_{\mathrm{DV}}\rangle_A$ to Bob through a lossy environment so that Bob receives a coherent-state qubit of the form

$$|\psi_{\mathrm{CV}}(\tau\alpha)\rangle_1 = N(a|\tau\alpha\rangle + b|-\tau\alpha\rangle)_1. \quad (26)$$

Note that state (2) is characterised by $\pm\alpha$ but state (26) by $\pm\tau\alpha$. This is because the initially prepared pure quantum channel state $\rho_{1234}(0) = |\Gamma(\alpha)\rangle_{1234} \langle\Gamma(\alpha)|$ has been decohered to be the mixed state $\rho_{1234}(\tau)$ given in eq. (25), i.e., the initial amplitudes $\pm\alpha$ of the coherent states are reduced to $\pm\tau\alpha$ at the time the task begins. Also, due to the dissipation, the normalisation factor in (26) is changed accordingly, namely, $N = N(a,b,\alpha) = (1 + 2Re(a^*b)\mathrm{e}^{-2\alpha^2})^{-1/2} \to N = N(a,b,\tau\alpha) = (1 + 2Re(a^*b)\mathrm{e}^{-2\tau^2\alpha^2})^{-1/2}$. The total state of Alice's DV qubit plus the dissipated quantum channel is $\rho_A\rho_{1234}(\tau)$ with $\rho_A = |\psi_{\mathrm{DV}}\rangle_A \langle\psi_{\mathrm{DV}}|$. In order to perform the hybrid-controlled teleportation in the Alice-to-Bob direction, each of the four parties should act properly as shown in figure 2.

Alice's actions. As a teleporter, Alice uses the optical device BS_{A4} to mix mode A and mode 4, then counts the photon numbers of those modes by two photodetectors D_A and D_4. Let the numbers of the counted photons respectively be n_A and n_4, then in terms of the dissipated quantum channel $\rho_{1234}(\tau)$, state of the remaining modes 1, 2 and 3 is of the form

$$\rho_{123}(\tau) = \frac{{}_{A4}\langle n_A, n_4|\mathrm{BS}_{A4}[\rho_A\rho_{1234}(\tau)]\mathrm{BS}^{+}_{A4}|n_A, n_4\rangle_{A4}}{P_{n_A,n_4}} \quad (27)$$

with

$$P_{n_A,n_4} = \mathrm{Tr}\left\{|n_A, n_4\rangle_{A4}\langle n_A, n_4|[\mathrm{BS}_{A4}[\rho_A\rho_{1234}(\tau)]\mathrm{BS}^{+}_{A4}]\right\} \quad (28)$$

the probability of co-counting n_A photons in mode A and n_4 photons in mode 4. After knowing the values of n_A and n_4, Alice, through an insecure yet reliable classical communication channel, publishes their values for Bob's later use. Note that each of mode A and mode 4 contains up to one photon and the beam-splitter is balanced so that there will be only five possible combinations of the values of $\{n_A, n_4\}$, which are $\{n_A, n_4\} = \{0,0\}, \{0,1\}, \{1,0\}, \{0,2\}$ and $\{2,0\}$.

David's actions. As a CV controller, David uses a photodetector D_2 to count the photon number in his mode 2, with the outcome n_2 to be also publicly announced for Bob's later use. Note that because mode 2 is a coherent state, $n_2 \in \{0, 1, 2, ..., \infty\}$ and can be classified as even and odd, i.e., $n_2 = \{\text{even,odd}\}$.

Charlie's actions. As a DV controller, Charlie first applies a Hadamard gate on her mode 3, then uses a photodetector D_3 to count the mode's photon number n_3,

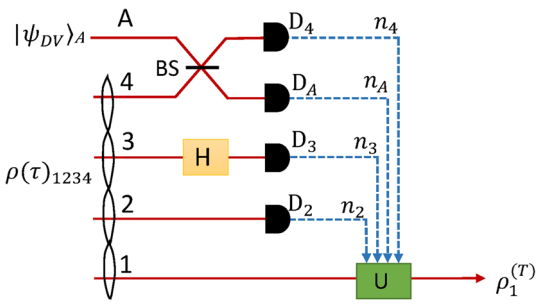

Figure 2. Scheme for controlled teleportation from a single-rail qubit to a coherent-state qubit using the dissipated quantum channel $\rho_{1234}(\tau)$ in eq. (25). BS denotes a beam-splitter, which acts on two modes as $\mathrm{BS}_{xy}(\pi/4) = \exp[\pi(a_x^+ a_y - a_y^+ a_x)/4]$. The solid line labelled 1 (2, 3, 4 and A) represents mode 1 (2, 3, 4 and A). D_2, D_3, D_A and D_4 are photodetectors to count the photon numbers in the corresponding modes. The dashed lines represent the numbers n_2, n_3, n_A and n_4 of the detected photons. H is the Hadamard gate. $U = X$ or XZ conditioned on the detected numbers of photons.

which she also discloses for Bob's later use. Note that $n_3 \in \{0, 1\}$ because mode 3 is a DV state spanned only by two number-states $|0\rangle$ and $|1\rangle$. Here the Hadamard gate for photonic single-rail quantum logic is non-trivial. A direct application of the Hadamard gate is impossible, but with photon counters and ancillae it turns out to be possible, yet succeeds very rarely [35]. However, it can be shown that use of photon counters and ancillae in combination with the adaptive phase measurements technique [32] allows the Hadamard gate to succeed half of the time. Assuming that the Hadamard gate is successfully applied, state of mode 1 at Bob's station after the actions of Alice, Charlie and David, is projected onto

$$\rho_1(\tau) = \frac{{}_{23}\langle n_2, n_3|H_3\rho_{123}(\tau)H_3^+|n_2, n_3\rangle_{23}}{Q_{n_2,n_3}} \tag{29}$$

with

$$Q_{n_2,n_3} = \mathrm{Tr}\{|n_2, n_3\rangle_{23}\langle n_2, n_3|[H_3\rho_{123}(\tau)H_3^+]\} \tag{30}$$

the probability of co-counting n_2 and n_3 photons in modes 2 and 3, respectively.

Bob's actions. As a receiver, Bob is the last one who should carry out some appropriate operation to reconstruct state $\rho_1(\tau)$ in eq. (29) to be a state closest to the desired state in eq. (26). As a rule, Bob has to make use of all the publicly published measurement outcomes n_A, n_4, n_3 and n_2 which may appear in 20 different combinations of $\{n_A, n_4, n_3, n_2\}$. In order to figure out which combination of $\{n_A, n_4, n_3, n_2\}$ is useful and which is not, we write down the explicit expression of $\rho_1(\tau)$ in eq. (29) as

$$\begin{aligned}\rho_1(\tau) = {} & (\delta_{0n_A}\delta_{1n_4}\delta_{0n_3} + \delta_{1n_A}\delta_{0n_4}\delta_{1n_3})\rho_1^{(1,n_2)}(\tau) \\ & + (\delta_{1n_A}\delta_{0n_4}\delta_{0n_3} + \delta_{0n_A}\delta_{1n_4}\delta_{1n_3})\rho_1^{(2,n_2)}(\tau) \\ & + \delta_{0n_A}\delta_{0n_4}(\delta_{0n_3} + \delta_{1n_3})\rho_1^{(3)}(\tau) \\ & + (\delta_{0n_A}\delta_{2n_4} + \delta_{2n_A}\delta_{0n_4})(\delta_{0n_3} + \delta_{1n_3})\rho_1^{(4)}(\tau),\end{aligned} \tag{31}$$

where

$$\begin{aligned}\rho_1^{(1,n_2)}(\tau) = {} & L^{(n_2)}(\tau)\{|b|^2|\tau\alpha\rangle_1\langle\tau\alpha| \\ & + (-1)^{n_2}C\tau^2(a^*b|\tau\alpha\rangle_1\langle-\tau\alpha| \\ & + ab^*|-\tau\alpha\rangle_1\langle\tau\alpha|) \\ & + [|b|^2(1-\tau^2) + |a|^2\tau^2]|-\tau\alpha\rangle_1\langle-\tau\alpha|\}\end{aligned} \tag{32}$$

with

$$\begin{aligned}L^{(n_2)}(\tau) = {} & [|b|^2(2-\tau^2) + |a|^2\tau^2 \\ & + (-1)^{n_2}C\tau^2(a^*b + b^*a)\mathrm{e}^{-2\alpha^2\tau^2}]^{-1},\end{aligned} \tag{33}$$

$$\rho_1^{(2,n_2)}(\tau) = \rho_1^{(1,n_2+1)}(\tau), \tag{34}$$

$$\rho_1^{(3)}(\tau) = \frac{|\tau\alpha\rangle_1\langle\tau\alpha| + (1-\tau^2)|-\tau\alpha\rangle_1\langle-\tau\alpha|}{2-\tau^2} \tag{35}$$

and

$$\rho_1^{(4)}(\tau) = |-\tau\alpha\rangle_1\langle-\tau\alpha|. \tag{36}$$

Clearly, from the above formulae, the measurement outcomes associated with the last two lines in eq. (31) are useless because neither $\rho_1^{(3)}(\tau)$ of eq. (35) nor $\rho_1^{(4)}(\tau)$ of eq. (36) contain informative parameters a and b, i.e., all the information to be teleported is totally lost. We have thus to deal only with the measurement outcomes associated with the first two lines in eq. (31).

Analysing eq. (32) indicates that when n_2 is even and $\tau = 1$ (the environment is dissipationless) $\rho_1^{(1,n_2)}(\tau)$ reduces to

$$\begin{aligned}\rho_1^{(1,\mathrm{even})}(\tau = 1) = {} & [1 + 2Re(a^*b)\mathrm{e}^{-2\alpha^2}]^{-1}\{|b|^2|\alpha\rangle_1\langle\alpha| \\ & + (a^*b|\alpha\rangle_1\langle-\alpha| + ab^*|-\alpha\rangle_1\langle\alpha|) \\ & + |a|^2|-\alpha\rangle_1\langle-\alpha|\} \\ = {} & X\,|\psi_{\mathrm{CV}}(\alpha)\rangle_1\,\langle\psi_{\mathrm{CV}}(\alpha)|\,X,\end{aligned} \tag{37}$$

from which it follows that

$$|\psi_{\mathrm{CV}}(\alpha)\rangle_1\,\langle\psi_{\mathrm{CV}}(\alpha)| = X\rho_1^{(1,\mathrm{even})}(\tau = 1)X. \tag{38}$$

In eqs (37) and (38) $|\psi_{\mathrm{CV}}(\alpha)\rangle$ is the CV qubit state defined in (2) and X denotes the so-called X-gate acting on coherent states as $X\,|\pm\tau\alpha\rangle = |\mp\tau\alpha\rangle$. Such an X-gate is nothing else but the π-phase-shift operation which is easily implemented by the phase-shifter $P(\pi)$.

Equality (38) tells us that the target state, $\rho_1^{(T)}(\tau)$, which is obtained by means of the hybrid controlled teleportation across the lossy environment at Bob's station should be

$$\rho_1^{(T)}(\tau) = X\rho_1^{(1,\text{even})}(\tau)X. \tag{39}$$

Now looking closer at the first two lines of eq. (31) we recognise that if the combinations of measurement outcomes $\{n_A, n_4, n_3, n_2\} = \{0, 1, 0, \text{even}\}$ or $\{1, 0, 1, \text{even}\}$ or $\{1, 0, 0, \text{odd}\}$ or $\{0, 1, 1, \text{odd}\}$ then $\rho_1(\tau)$ reduces to $\rho_1^{(1,\text{even})}(\tau) = \rho_1^{(2,\text{odd})}(\tau) = X\rho_1^{(T)}(\tau)X$. This means that $\rho_1^{(T)}(\tau) = X\rho_1^{(1,\text{even})}(\tau)X$, i.e., the target state can be reconstructed from $\rho_1^{(1,\text{even})}(\tau)$ or $\rho_1^{(2,\text{odd})}(\tau)$ by applying the X-gate on mode 1. As the X-gate implementation on coherent states is deterministic, the probability for this event to occur, in terms of the probabilities P_{n_A,n_4} and Q_{n_2,n_3} defined in eqs (28) and (30), reads as

$$\begin{aligned} P_X =& \frac{1}{2}[P_{0,1}\left(Q_{0,\text{even}} + Q_{1,\text{odd}}\right) \\ &+ P_{1,0}\left(Q_{1,\text{even}} + Q_{0,\text{odd}}\right)] \\ =& \frac{1}{8}[|b|^2(2-\tau^2) + |a|^2\tau^2 \\ &+ C\tau^2(a^*b + b^*a)\mathrm{e}^{-2\tau^2\alpha^2}], \end{aligned} \tag{40}$$

where the factor $1/2$ in the first line of eq. (40) accounts for the probability of Charlie's successful application of the Hadamard gate. Otherwise, if the combinations of measurement outcomes $\{n_A, n_4, n_3, n_2\} = \{0, 1, 0, \text{odd}\}$ or $\{1, 0, 1, \text{odd}\}$ or $\{1, 0, 0, \text{even}\}$ or $\{0, 1, 1, \text{even}\}$, then $\rho_1(\tau)$ reduces to $\rho_1^{(1,\text{odd})}(\tau) = \rho_1^{(2,\text{even})}(\tau) = XZ\rho_1^{(T)}(\tau)ZX$. This implies that to obtain the target state $\rho_1^{(T)}(\tau)$, Bob should apply on $\rho_1^{(1,\text{odd})}(\tau)$ or $\rho_1^{(2,\text{even})}(\tau)$ the XZ-gate, where the so-called Z-gate transforms $|\pm\tau\alpha\rangle$ to $\pm|\pm\tau\alpha\rangle$. The problem is that for coherent states that constitute an over-complete set of states, implementation of such Z-gate is difficult. To circumvent the difficulty, one may approximate the gate by utilising the displacement operator [36] or by trickily resorting to teleportation-assisted techniques [37] or by subtracting one photon from the coherent state [38]. Anyway, implementation of the Z-gate on a coherent state is non-deterministic. On an average, two attempts are needed per Z-gate, i.e., the probability of successful application of the Z-gate is 50% (see also ref. [37]). Hence, this event happens with the probability

$$\begin{aligned} P_{XZ} =& \frac{1}{4}[P_{0,1}\left(Q_{0,\text{odd}} + Q_{1,\text{even}}\right) \\ &+ P_{1,0}\left(Q_{1,\text{odd}} + Q_{0,\text{even}}\right)] \\ =& \frac{1}{16}[|b|^2(2-\tau^2) + |a|^2\tau^2 \\ &- C\tau^2(a^*b + b^*a)\mathrm{e}^{-2\tau^2\alpha^2}], \end{aligned} \tag{41}$$

where the factor $1/4$ in the first line of eq. (41) accounts for the probability of both Charlie's successful application of the Hadamard gate and Bob's successful application of the Z-gate. The total success probability $P_{\text{DV}\to\text{CV}}$ for teleporting the single-rail qubit state $|\psi_{\text{DV}}\rangle_A$ of eq. (1) to the target CV qubit state $\rho_1^{(T)}(\tau)$ of eq. (39) is given by

$$\begin{aligned} P_{\text{DV}\to\text{CV}} =& P_X + P_{XZ} \\ =& \frac{1}{16}[3(|b|^2(2-\tau^2) + |a|^2\tau^2) \\ &+ C\tau^2(a^*b + b^*a)\mathrm{e}^{-2\tau^2\alpha^2}]. \end{aligned} \tag{42}$$

The fidelity $F_{\text{DV}\to\text{CV}}$ between the obtained target state $\rho_1^{(T)}(\tau)$ in eq. (39) and the intended one $|\psi_{\text{CV}}(\tau\alpha)\rangle_1$ in eq. (26) is mathematically determined by

$$\begin{aligned} F_{\text{DV}\to\text{CV}} =& \ {}_1\langle\psi_{\text{CV}}(\tau\alpha)|\rho_1^{(T)}(\tau)|\psi_{\text{CV}}(\tau\alpha)\rangle_1 \\ =& N^2(a,b,\tau\alpha)L^{(\text{even})}(\tau)\{|b(b+a\mathrm{e}^{-2\tau^2\alpha^2})|^2 \\ &+((1-\tau^2)|b|^2 + \tau^2|a|^2)|(b\mathrm{e}^{-2\tau^2\alpha^2} + a)|^2 \\ &+2C\tau^2 Re[ab^*(a\mathrm{e}^{-2\tau^2\alpha^2}+b)(a^*+b^*\mathrm{e}^{-2\tau^2\alpha^2})]\}. \end{aligned} \tag{43}$$

4.2 *Controlled teleportation from a coherent-state qubit to a single-rail qubit*

In this subsection, we deal with the second task formulated in §2. Now Bob plays the role of a teleporter holding a coherent-state qubit in the CV state $|\psi_{\text{CV}}(\tau\alpha)\rangle_B = N(a|\tau\alpha\rangle + b|-\tau\alpha\rangle)_B$ with parameters a and b unknown to him. Bob's task is to securely transfer to Alice the DV state of a single-rail qubit of the form $|\psi_{\text{DV}}\rangle_4 = (a|0\rangle + b|1\rangle)_4$. The actions of the four parties in this case are shown in figure 3.

As in the first task, the four parties shared beforehand the same dissipated quantum channel characterised by the density matrix $\rho_{1234}(\tau)$ in eq. (25) with the same distribution of modes. The actions of the controllers Charlie and David are not changed, but those of Alice and Bob are. That is, Bob now acts first by superimposing mode 1 and mode B on a BS_{1B} followed by detecting the photon numbers of the outgoing modes by photodetectors D_1 and D_B, which register n_1 and n_B photons, respectively, with $n_1, n_B \in \{0, \text{even} \neq 0, \text{odd}\}$. If the photon numbers registered by Charlie's photodetector D_3 and David's photodetector D_2 are $n_3 \in \{0, 1\}$ and

$n_2 \in \{\text{even, odd}\}$, respectively, then the quantum channel collapses to Alice's mode 4 as

$$\rho_4(\tau) = \frac{{}_{321B}\langle n_3, n_2, n_1, n_B|\rho_{1234B}(\tau)|n_3, n_2, n_1, n_B\rangle_{321B}}{P_{n_3,n_2,n_1,n_B}}, \tag{44}$$

where

$$\rho_{1234B}(\tau) = H_3 \mathrm{BS}_{1B}\rho(\tau)_{1234}\rho_B(\tau)\mathrm{BS}^{+}_{1B}H^{+}_3, \tag{45}$$

with

$$\rho_B(\tau) = |\psi_{\mathrm{CV}}(\tau\alpha)\rangle_B\,\langle\psi_{\mathrm{CV}}(\tau\alpha)|$$

and

$$P_{n_3,n_2,n_1,n_B} = \mathrm{Tr}\{|n_3, n_2, n_1, n_B\rangle_{321B}\langle n_3, n_2, n_1, n_B| \otimes \rho_{1234B}(\tau)\} \tag{46}$$

the probability of co-registering n_3, n_2, n_1 and n_B photons in modes 3, 2, 1 and B, respectively. Substituting $\rho_{1234}(\tau)$ in eq. (25) and $\rho_B(\tau)=|\psi_{\mathrm{CV}}(\tau\alpha)\rangle_B\,\langle\psi_{\mathrm{CV}}(\tau\alpha)|$ with $|\psi_{\mathrm{CV}}(\tau\alpha)\rangle$ defined by eq. (26) into eq. (45) and then into eq. (44) we arrive at

$$\begin{aligned}\rho_4(\tau) = {}& \delta_{0n_3}\delta_{0n_B}\rho_4^{(1,n_1+n_2)}(\tau) + \delta_{1n_3}\delta_{0n_B}\rho_4^{(2,n_1+n_2)}(\tau)\\ &+ \delta_{0n_3}\delta_{0n_1}\rho_4^{(3,n_2+n_B)}(\tau) + \delta_{1n_3}\delta_{0n_1}\rho_4^{(4,n_2+n_B)}(\tau)\\ &+ \delta_{0n_B}\delta_{0n_1}(\delta_{0n_3}+\delta_{1n_3})\rho_4^{(5)}(\tau),\end{aligned} \tag{47}$$

where

$$\begin{aligned}\rho_4^{(1,n_1+n_2)}(\tau) = {}& \{(|a|^2 + |b|^2(1-\tau^2))|0\rangle_4\langle 0|\\ &+ (-1)^{(n_1+n_2)}C\tau^2(ab^*|0\rangle_4\langle 1| + ba^*|1\rangle_4\langle 0|)\\ &+ |b|^2\tau^2|1\rangle_4\langle 1|\},\ n_1 \neq 0,\end{aligned} \tag{48}$$

$$\rho_4^{(2,n_1+n_2)}(\tau) = \rho_4^{(1,n_1+n_2+1)}(\tau), \tag{49}$$

$$\begin{aligned}\rho_4^{(3,n_2+n_B)}(\tau) = {}& \{(|b|^2 + |a|^2(1-\tau^2))|0\rangle_4\langle 0|\\ &+ (-1)^{(n_2+n_B)}C\tau^2(ba^*|0\rangle_4\langle 1| + ab^*|1\rangle_4\langle 0|)\\ &+ |a|^2\tau^2|1\rangle_4\langle 1|\},\ n_B \neq 0,\end{aligned} \tag{50}$$

$$\rho_4^{(4,n_2+n_B)}(\tau) = \rho_4^{(3,n_2+n_B+1)}(\tau) \tag{51}$$

and

$$\begin{aligned}\rho_4^{(5)}(\tau) = {}& \frac{1}{2}[(2-\tau^2))|0\rangle_4\langle 0|\\ &+ C\tau^2(|0\rangle_4\langle 1| + |1\rangle_4\langle 0|) + \tau^2|1\rangle_4\langle 1|].\end{aligned} \tag{52}$$

Since the parameters a and b disappear in $\rho_4^{(5)}(\tau)$ of eq. (52), we disregard the last term in the right-hand side of eq. (47) and concentrate only on the rest of the terms. As can be examined from eq. (48), when n_1+n_2 is even (i.e., either $\{n_1 = \text{even} \neq 0, n_2 = \text{even}\}$ or $\{n_1 = \text{odd}, n_2 = \text{odd}\}$) and $\tau = 1$ (i.e., there is no dissipation), $\rho_4^{(1,n_1+n_2)}(\tau)$ simplifies to

$$\begin{aligned}\rho_4^{(1,\text{even})}(\tau=1) = {}& \rho_4^{(2,\text{odd})}(\tau=1)\\ = {}& \{|a|^2|0\rangle_4\langle 0| + |b|^2|1\rangle_4\langle 1|\\ &+ (ab^*|0\rangle_4\langle 1| + ba^*|1\rangle_4\langle 0|)\}\\ = {}& |\psi_{DV}\rangle_4\,\langle\psi_{DV}|\,.\end{aligned} \tag{53}$$

This suggests that the DV target state $\rho_4^{(T)}(\tau)$ at Alice's station at a given $\tau \neq 1$ should be

$$\rho_4^{(T)}(\tau) = \rho_4^{(1,\text{even})}(\tau) = \rho_4^{(2,\text{odd})}(\tau). \tag{54}$$

Having identified the DV target state, we are in the position to analyse all the possible happening events conditioned on the measurement outcomes $\{n_3, n_2, n_1, n_B\}$. To have an overview, we summarise the results of the analysis in table 1.

Table 1 shows that to obtain the target state $\rho_4^{(T)}(\tau)$, Alice needs to (i) do nothing in cases #1, #2, #3, #4, (ii) implement an Z-gate in cases #5, #6, #7, #8, (iii) implement an X-gate in cases #9, #10, #11, #12 and (iv) implement an XZ-gate in cases #13, #14, #15, #16. As commented in §2, for single-rail qubits, the Z-gate is trivial while the X-gate is non-trivial but can be done with a probability of 1/2. The total success probability of the hybrid controlled teleportation from $|\psi_{\mathrm{CV}}(\tau\alpha)\rangle$ to $|\psi_{\mathrm{DV}}\rangle$ is then

$$P_{\mathrm{CV}\to\mathrm{DV}} = \frac{1}{2}\sum_{k=0,1}\sum_{l=\text{even,odd}}\sum_{m=\text{even}\neq 0,\text{odd}}\left(P_{k,l,m,0} + \frac{1}{2}P_{k,l,0,m}\right), \tag{55}$$

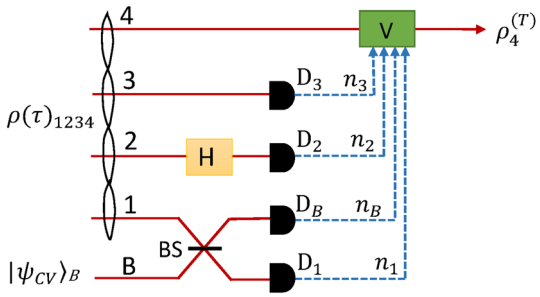

Figure 3. Scheme for controlled teleportation from a coherent-state qubit to a single-rail qubit using the dissipated quantum channel $\rho_{1234}(\tau)$ in eq. (25). BS denotes a beam-splitter, which acts on two modes as $\mathrm{BS}_{xy}(\pi/4) = \exp[\pi(a_x^+a_y - a_y^+a_x)/4]$. The solid line labelled B (1, 2, 3 and 4) represents mode B (1, 2, 3 and 4). D_1, D_B, D_2 and D_3 are photodetectors to count the photon numbers in the corresponding modes. The dashed lines represent the numbers n_1, n_B, n_2 and n_3 of the detected photons. H is the Hadamard gate. $V = I, X, Z$ or XZ conditioned on the detected numbers of photons.

Table 1. The collapsed state of $\rho_4(\tau)$ in eq. (47) conditioned on the 16 possible cases of the measurement outcomes $\{n_3, n_2, n_1, n_B\}$. The states $\rho_4^{(j,\text{even})}(\tau)$, $\rho_4^{(j,\text{odd})}(\tau)$ with $j = 1, 2, 3, 4$ and $\rho_4^{(T)}(\tau)$ are given in eqs (48)–(51) and (54), respectively.

Case #	n_3	n_2	n_B	n_1	$\rho_4(\tau)$
1, 2	0, 0	even, odd	0, 0	even $\neq 0$, odd	$\rho_4^{(1,\text{even})}(\tau) = \rho_4^{(T)}(\tau)$
3, 4	1, 1	even, odd	0, 0	odd, even $\neq 0$	$\rho_4^{(2,\text{odd})}(\tau) = \rho_4^{(T)}(\tau)$
5, 6	0, 0	even, odd	0, 0	odd, even $\neq 0$	$\rho_4^{(1,\text{odd})}(\tau)$ $Z\rho_4^{(T)}(\tau)Z$
7, 8	1, 1	even, odd	0, 0	even $\neq 0$, odd	$\rho_4^{(2,\text{even})}(\tau) = Z\rho_4^{(T)}(\tau)Z$
9, 10	0, 0	even, odd	even $\neq 0$, odd	0, 0	$\rho_4^{(3,\text{even})}(\tau) = X\rho_4^{(T)}(\tau)X$
11, 12	1, 1	even, odd	odd, even $\neq 0$	0, 0	$\rho_4^{(4,\text{odd})}(\tau) = X\rho_4^{(T)}(\tau)X$
13, 14	0, 0	even, odd	odd, even $\neq 0$	0, 0	$\rho_4^{(3,\text{odd})}(\tau)$ $XZ\rho_4^{(T)}(\tau)ZX$
15, 16	1, 1	even, odd	even $\neq 0$, odd	0, 0	$\rho_4^{(4,\text{even})}(\tau) = XZ\rho_4^{(T)}(\tau)ZX$

with P_{n_3,n_2,n_1,n_B} given by eq. (46). In the above formula the common factor $1/2$ stands for the probability of the Hadamard gate implementation on mode 3 and the other factor $1/2$ inside the parentheses for implementation of the X-gate on mode 4. Calculating analytical expressions of P_{n_3,n_2,n_1,n_B} in (46) and substituting them into eq. (55), we get explicitly

$$P_{\text{CV}\to\text{DV}} = \frac{3}{8}\frac{1 - \mathrm{e}^{-2\tau^2\alpha^2}}{1 + 2Re(a^*b)\mathrm{e}^{-2\tau^2\alpha^2}}. \tag{56}$$

The fidelity between the obtained target state $\rho_4^{(T)}(\tau)$ and the intended state (1) is

$$\begin{aligned} F_{\text{CV}\to\text{DV}} =& {}_4\langle\psi_{\text{DV}}|\rho_4^{(T)}(\tau)|\psi_{\text{DV}}\rangle_4 \\ =& |a|^4 + \tau^2|b|^4 + (1 - \tau^2 + 2C\tau^2)|a|^2|b|^2. \end{aligned} \tag{57}$$

5. Discussion

As it should be, in the absence of photon losses the mixed state $\rho_{1234}(\tau)$ in eq. (25) of the quantum channel is simplified to a pure state $\rho_{1234}(\tau = 1) = |\Gamma\rangle_{1234}\langle\Gamma|$, with $|\Gamma\rangle_{1234}$ given in eq. (3). So the fidelity $F_{\text{DV}\to\text{CV}}$ of teleportation from a single-rail qubit to a coherent-state qubit is equal to 1. In the opposite limit, when total photon loss occurs, the quantum channel is completely dissipated, i.e., $\rho_{1234}(\tau)$ becomes $\rho_{1234}(\tau = 0) = |0, 0, 0, 0\rangle_{1234}\langle 0, 0, 0, 0|$. In the same limit (i.e., $\tau \to 0$) the to-be-teleported CV state (26) also becomes the vacuum one $|0\rangle_1$. Since in this limit all the modes are disentangled from each other, what is done with modes 2, 3, 4 and A does not have any influence on the state of mode 1, which remains in $|0\rangle_1$. Hence, the corresponding fidelity is *formally* also equal to 1, as in the case of no photon losses ('formally' because such a unit fidelity is just due to the mathematical definition but the target state contains no information at all of the intended state, i.e., it is useless physically). As fidelity cannot exceed 1, in the course of dimensionless time γt evolving from $\gamma t = 0$ to ∞ (tantamount to τ varying from 1 to 0) there must exist a minimum fidelity. Such behaviour of time-dependent fidelity is in fact observed by the numerical calculation. We illustrate this in figure 4 where the fidelity $F_{\text{DV}\to\text{CV}}$ for a particular case of teleporting the DV equally-weighted state $(|0\rangle + |1\rangle)/\sqrt{2}$ to an even Schrödinger cat state $N(|\tau\alpha\rangle + |-\tau\alpha\rangle)$ is plotted vs. γt for several values of α. For a given α, as time moves the fidelity is first quickly decreasing to reach a minimum value, then slowly increasing to saturate to 1 for a large enough period of time (say, for $t \geq 10/\gamma$). Also visualized is the fact that the smaller the value of α the shallower the bottom of the fidelity curve.

For teleportation in the opposite direction, i.e., from a coherent-state qubit to a single-rail one, a different behaviour of fidelity is observed. Although $F_{\text{CV}\to\text{DV}} = 1$ at $\gamma t = 0$, it is not so in the long-time limit. Actually,

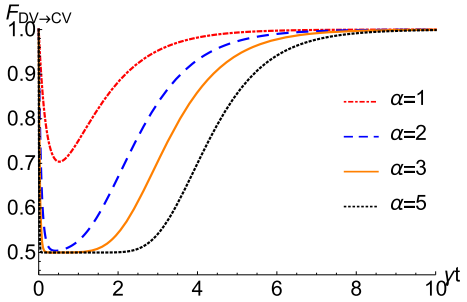

Figure 4. The fidelity of controlled teleportation from a single-rail qubit in the specific state $(|0\rangle + |1\rangle)/\sqrt{2}$ to the even Schrödinger cat state $N(|\tau\alpha\rangle + |-\tau\alpha\rangle)$ as a function of the scaled dimensionless time γt with $\alpha = 1$ (red dash–dotted curve), $\alpha = 2$ (blue dashed curve), $\alpha = 3$ (orange solid curve) and $\alpha = 5$ (black dotted curve).

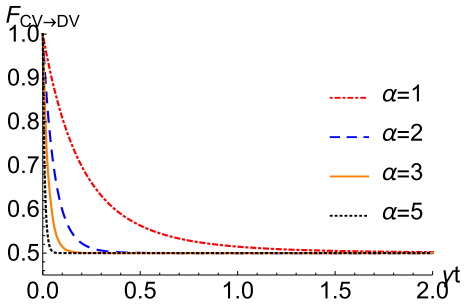

Figure 5. The fidelity of controlled teleportation from the even Schrödinger cat state $N(|\tau\alpha\rangle + |-\tau\alpha\rangle)$ to a single-rail qubit in the specific state $(|0\rangle + |1\rangle)/\sqrt{2}$ as a function of the scaled dimensionless time γt with $\alpha = 1$ (red dash–dotted curve), $\alpha = 2$ (blue dashed curve), $\alpha = 3$ (orange solid curve) and $\alpha = 5$ (black dotted curve).

in the limit of $\gamma t \to \infty$ (tantamount to $\tau \to 0$) the DV intended state at Alice's station is intact, $|\psi_{DV}\rangle = a\,|0\rangle + b\,|1\rangle$, in spite of full disentanglement of the quantum channel: all its modes turn out to be the vacuum states. Thus, the squared overlap between the vacuum state of mode 4 and the intended state $|\psi_{DV}\rangle$ is taken as the corresponding fidelity, which is mathematically calculated to be equal to $|a|^2$. Since $|a|^2 < 1$ for the general DV state, the fidelity $F_{CV\to DV}$, unlike $F_{DV\to CV}$, may not experience a minimum. This is reflected in figure 5 which displays the fidelity $F_{CV\to DV}$ vs. γt for teleporting an even Schrödinger cat state $N(|\tau\alpha\rangle + |-\tau\alpha\rangle)$ to the single-rail state $(|0\rangle + |1\rangle)/\sqrt{2}$. Figure 5 shows that for a given α the fidelity $F_{CV\to DV}$ starts from 1 at $\gamma t = 0$, then quickly decreases as γt grows without dropping below $1/2$ but saturates to that minimum value for $t \geq 2/\gamma$. The rate of decrease of fidelity grows with increasing α.

Now we notice the issue that, unlike teleportation in lossless environments, where both the success probability and fidelity are independent of the input states, here the dissipation effect gives rise to their dependence on the informative parameters a and b of the state to be teleported. Of interest is then the average over all possible values of the input parameters. Recalling that a and b are bound by the constraint $|a|^2 + |b|^2 = 1$ and a quantum state is physical up to a global phase factor, we can adopt the following parametrisation $a = \cos\theta$ and $b = \mathrm{e}^{i\varphi}\sin\theta$, with $0 \leq \theta \leq \pi/2$ and $0 \leq \varphi \leq 2\pi$. Assuming a uniform probability density, $(2\pi)^{-1}$, for φ distribution and that for θ distribution is $\sin(2\theta)$, the average of any function $f(\theta, \varphi)$ is given by [39].

$$\overline{f}(\theta,\varphi) = \frac{1}{2\pi}\int_0^{2\pi} \mathrm{d}\varphi \int_0^{\pi/2} f(\theta,\varphi)\sin(2\theta)\mathrm{d}\theta. \quad (58)$$

By virtue of formula (58) and using eqs (42) and (56) we explicitly derive the corresponding average success probabilities as

$$\overline{P}_{DV\to CV} = \frac{3}{16} \quad (59)$$

and

$$\overline{P}_{CV\to DV} = \frac{3(1-\mathrm{e}^{-2\tau^2\alpha^2})\,\mathrm{arctanh}(\mathrm{e}^{-2\tau^2\alpha^2})}{8\mathrm{e}^{-2\tau^2\alpha^2}}. \quad (60)$$

As for the average fidelities, the averaging integration (58) for $F_{DV\to CV}$ of eq. (43) is hardly to be taken analytically to obtain an explicit expression for $\overline{F}_{DV\to CV}$. So we shall numerically calculate it. As for $F_{CV\to DV}$, eq. (57) for it is quite simple and the averaging integration is straightforward yielding

$$\overline{F}_{CV\to DV} = \frac{1}{2} + \frac{1}{6}\tau^2(1 + 2\mathrm{e}^{-4(1-\tau^2)\alpha^2}). \quad (61)$$

For easy comparison, we plot in the same figure (figure 6) both the average fidelities $\overline{F}_{DV\to CV}$ and $\overline{F}_{CV\to DV}$ as functions of γt for four different values of α. Qualitatively, the fidelities behave much like those for the particular case with $a = b = 1/\sqrt{2}$ (or the same $\varphi = 0$ and $\theta = \pi/4$) shown in figures 4 and 5. That is, for a given α, $\overline{F}_{DV\to CV}$ suffers a minimum before approaching 1, while $\overline{F}_{CV\to DV}$ monotonically decreases and asymptotically tends to its lowest value of $1/2$, which is the average value of $F_{CV\to DV}(\gamma t \to \infty) = \cos^2(\theta)$. Remarkably, for all values of α, $\overline{F}_{DV\to CV}$ is greater than $\overline{F}_{CV\to DV}$ during the entire time evolution. Furthermore, for small values of α (say, $\alpha = 0.5$ as in figure 6a) quantum teleportation from single-rail qubit to coherent-state qubit always outperforms the corresponding classical teleportation whose best fidelity is $2/3$ (represented by a dashed horizontal line in figure 6). For bigger values of α (e.g., $\alpha = 1, 2$ and 5 as in figures 6b, 6c and 6d, respectively) there may exist a 'window of time' within which $\overline{F}_{CV\to DV} < 2/3$, i.e., quantum teleportation turns out

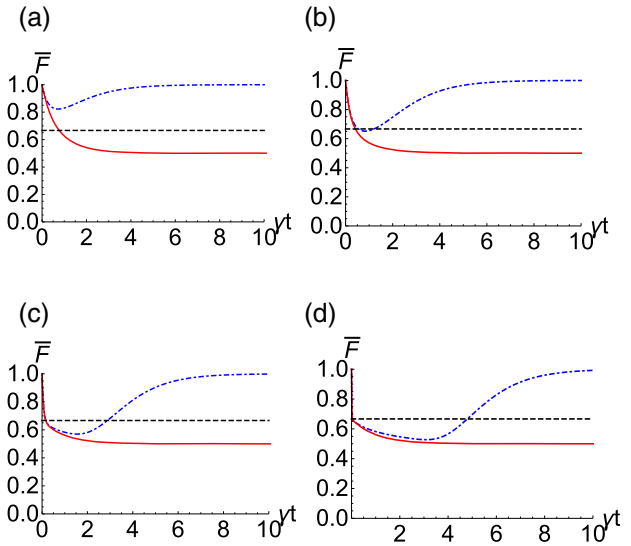

Figure 6. The average fidelity of controlled teleportation from a single-rail qubit to a coherent-state qubit (blue dash—dotted curves) and from a coherent-state qubit to a single-rail qubit (red solid curves) as a function of the scaled dimensionless γt with (**a**) $\alpha = 0.5$, (**b**) $\alpha = 1$, (**c**) $\alpha = 2$ and (**d**) $\alpha = 5$. The back horizontal dashed line at $2/3$ is the best achievable classical fidelity.

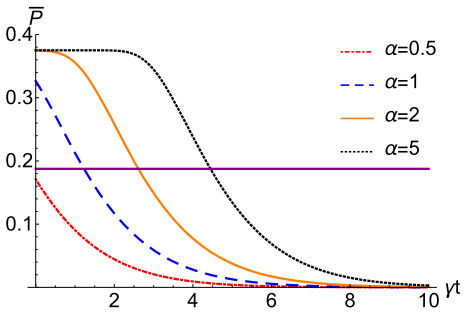

Figure 7. The average success probability of controlled teleportation from a coherent-state qubit to a single-rail qubit as a function of the scaled dimensionless γt with $\alpha = 0.5$ (red dash-dotted curve), $\alpha = 1$ (blue dashed curve), $\alpha = 2$ (orange solid curve) and $\alpha = 5$ (black dotted curve). The average success probability from a single-rail qubit to a coherent-state qubit is constant and represented by a purple horizontal line at $3/16$.

worse than classical one. Concerning quantum teleportation from coherent-state qubit to single-rail qubit it is better than classical one only for a short initial duration of time as $\overline{F}_{\mathrm{CV}\to\mathrm{DV}}$ quickly becomes smaller than $2/3$ and remains so later on. This qualitative property holds independent of α. Yet, quantitatively, a larger value of α narrows the initial time duration of the advantage of quantum over classical teleportation.

The average success probabilities are displayed in figure 7. While quantum teleportation from single-rail qubit to coherent-state qubit succeeds with a constant probability $\overline{P}_{\mathrm{DV}\to\mathrm{CV}} = 3/16$, quantum teleportation from coherent-state qubit to single-rail will succeed with a probability $\overline{P}_{\mathrm{CV}\to\mathrm{DV}}$ which is subject to α and can be made greater than $\overline{P}_{\mathrm{DV}\to\mathrm{CV}}$. For example, if α is quite small then $\overline{P}_{\mathrm{CV}\to\mathrm{DV}} < \overline{P}_{\mathrm{DV}\to\mathrm{CV}}$ all the time (see the curve with $\alpha = 0.5$ in figure 7). Nevertheless, when α is getting bigger, $\overline{P}_{\mathrm{CV}\to\mathrm{DV}}$ may become greater than $\overline{P}_{\mathrm{DV}\to\mathrm{CV}}$ for not too large γt. The interval of γt in which $\overline{P}_{\mathrm{CV}\to\mathrm{DV}} > \overline{P}_{\mathrm{DV}\to\mathrm{CV}}$ widens with increasing α, as seen from the curves with $\alpha = 1$, 2 and 5 in figure 7.

6. Conclusion

In conclusion, we have first suggested a scheme to prepare an appropriate hybrid four-party pure entangled state of the form (3), which after the sharing process among the four authorised parties through a lossy environment is dissipated and becomes a mixed one as given in eq. (25). We then use this mixed state as the working quantum channel to perform controlled teleportations between a single-rail and a coherent-state qubits. Because of the dissipation effect, the teleportations' fidelities and success probabilities are state-dependent. So we calculate their averages which are state-independent. With respect to the average fidelity, teleportation from a single-rail qubit to a coherent-state qubit always outperforms that in the opposite direction from a coherent-state qubit to a single-rail qubit. However, it turns other way around with respect to the average success probability which is constant for teleportation from a coherent-state qubit to a single-rail qubit but rather flexible in terms of α in the opposite direction. The α-dependence specifically appears in macroscopic superpositions/entanglements and here it causes quite subtle affects. For instance, an increase in α lowers the average fidelities (see figures 4–6) but rises the average success probability (as seen from figure 7). It is worthy to note that single-rail encoding is particularly interesting due to its natural interconvertibility between different physical systems such as atomic, mechanical and optical systems. The single-rail qubit can also be seamlessly converted into other qubit formats, for example, polarisation qubits [40]. This means that the hybrid entanglement between a coherent state and a polarisation qubit state can be generated from the hybrid entanglement between coherent states and single-rail states.

The idea of controlled teleportations within a DV [41] as well as a CV [42] homogeneous network was

put forward before. Here this idea is deployed to the case of a heterogeneous network. The choice of two controllers of different abilities as in this paper is not accidental. In fact, it matters. One may think of Alice and Charlie (Bob and David) as belonging to the same company working with DV (CV) toolkits and Charlie (David) is the boss of Alice (Bob). It would be biased in favour of the DV (CV) company if only Charlie (David) supervises the task. So, to ensure a fair affair for the two companies, both Charlie and David should operate as equal-right controllers: declining cooperation of either of them prevents completion of the hybrid teleportation tasks. However, their powers might not be identical. Our protocols would work better for larger values of α because then $|\langle+\alpha| - \alpha\rangle| = \exp(-2|\alpha|^2)$ gets smaller and for a sufficiently large α, say, $\alpha \geq 2$ the states $|+\alpha\rangle$ and $|-\alpha\rangle$ become orthogonal to each other which serve very well as two basis vectors of a two-dimensional space. A large value of α also slows down the rate at which $|\pm\tau\alpha\rangle$ tends to $|0\rangle$ when τ tends to 0 making the protocols more robust against the decoherence. The coherent-state qubit in eq. (2) with a large value of α can be produced by several techniques thanks to advanced quantum technology (see, e.g., [43–45]). Our proposed schemes would work well beyond the ideal regime because practical non-ideal issues such as decoherence due to lossy environment and effect due to detector inefficiency have been taken into account. We plan in a subsequent work, to analyse in detail the power of each of the controllers (the DV one as well as the CV one) in these particular hybrid teleportation protocols by calculating the fidelity that is obtained without the cooperation of one controller or the other. We also intend to study other types of DV and CV encodings as well as possible hybrid DV–CV encodings and try to devise ways of controllable transfer of quantum information contained in those various encodings within complex heterogeneous quantum networks.

Acknowledgements

Cao Thi Bich was funded by Vingroup Joint Stock Company and supported by the Domestic Master/Ph.D. Scholarship Programme of Vingroup Innovation Foundation (VINIF), Vingroup Big Data Institute (VINBIGDATA), code VINIF.2020.TS.49.

References

[1] M A Nielsen and I L Chuang, *Quantum computation and quantum information* (Cambridge University Press, Cambridge, UK, 2000)
[2] E Knill, L Laflamme and G J Milburn, *Nature* **46**, 409 (2001)
[3] P Kok, W J Munro, K Nemoto, T C Ralph, J P Dowling and G J Milburn, *Rev. Mod. Phys.* **79**, 135 (2007)
[4] S L Braunstein and A Pati (eds) *Continuous variable quantum information* (Kluwer Academic, 2003)
[5] S L Braunstein and P van Loock, *Rev. Mod. Phys.* **77**, 513 (2005)
[6] S Choudhury and P K Panigrahi, *AIP Conf. Proc*. **1384**, 91 (2011)
[7] N Lütkenhaus, J Calsamiglia and K A Suominen, *Phys. Rev. A* **59**, 3245 (1999)
[8] D Bouwmeester, J W Pan, K Mattle, M Eible, H Weinfurter and A Zeilinger, *Nature* **390**, 575 (1997)
[9] D Boschi, S Branca, F De Martini, L Harcy and S Popescu, *Phys. Rev. Lett.* **80**, 1121 (1998)
[10] H Jeong, M S Kim and J Lee, *Phys. Rev. A* **64**, 052308 (2001)
[11] H Prakash, N Chandra, R Prakash and Shivani, *Phys. Rev. A* **75**, 044305 (2007)
[12] T B Pittman, M J Fitch, B C Jacobs and J D Franson, *Phys. Rev. A* **68**, 032316 (2003)
[13] S L Braunstein and H J Kimble, *Phys. Rev. Lett*. **80**, 869 (1998)
[14] K Park and H Jeong, *Phys. Rev. A* **82**, 062325 (2010)
[15] S W Lee and H Jeong, *Phys. Rev. A* **87**, 022326 (2013)
[16] O Morin, J D Bancal, M Ho, P Sekatski, V D'Auria, N Gisin, J Laurat and N Sangouard, *Phys. Rev. Lett.* **110**, 130401 (2013)
[17] A Furusawa and P van Loock, *Quantum teleportation and entanglement: A hybrid approach to optical quantum information processing* (Wiley-VCH, Weinheim, 2011)
[18] K Nemoto and W J Munro, *Phys. Rev. Lett.* **93**, 250502 (2004)
[19] W J Munro, K Nemoto and T P Spiller, *New J. Phys.* **7**, 137 (2005)
[20] H Jeong, *Phys. Rev. A* **72**, 034305 (2005)
[21] H Jeong, *Phys. Rev. A* **73**, 052320 (2006)
[22] P van Loock, W J Munro, K Nemoto, T P Spiller, T D Ladd, S L Braunstein and G J Milb, *Phys. Rev. A* **78**, 022303 (2008)
[23] P van Loock, *Laser Photon. Rev.* **5**, 167 (2011)
[24] O Morin, K Huang, J Liu, H L Jeannic, C Fabre and J Laurat, *Nat. Photon.* **8**, 570 (2014)
[25] H Jeong, A Zavatta, M Kang, S W Lee, L S Costanzo, S Grandi, C Ralph and M Bellini, *Nat. Photon.* **8**, 564 (2014)
[26] L S Costanzo, A Zavatta, S Grandi, M Bellini, H Jeong, M Kang, S W Lee and T C Ralph, *Phys. Scr.* **90**, 074045 (2015)
[27] W Son, M S Kim, L Lee and D Ahn, *J. Mod. Opt.* **49**, 1739 (2002)
[28] M Paternostro, W Son and M S Kim, *Phys. Rev. Lett.* **92**, 197901 (2004)
[29] U L Andersen, J S Neergaard-Nielsen, P van Loock and A Furusawa, *Nat. Phys.* **11**, 713 (2015)

[30] J Eisert, S Scheel and M B Plenio, *Phys. Rev. Lett.* **89**, 137903 (2002)
[31] P Park, S W Lee and H Jeong, *Phys. Rev. A* **86**, 062301 (2012)
[32] T C Ralph, A P Lund and H M Wiseman, *J. Opt. B: Quantum Semiclass. Opt.* **7**, S245 (2005)
[33] H Jeong, S L Bae and S Choi, *Quant. Inf. Process.* **15**, 913 (2016)
[34] W H Louisell, *Quantum statistical properties of radiation* (Wiley, New York, 1997)
[35] A P Lund and T C Ralph, *Phys. Rev. A* **66**, 032307 (2002)
[36] H Jeong and M S Kim, *Phys. Rev. A* **65**, 042305 (2002)
[37] N B An, K Kim and J Kim, *Phys. Lett. A* **375**, 245 (2011)
[38] N Horiuchi, *Nat. Photon.* **11**, 532 (2017)
[39] K Zyczkowski and H J Sommers, *J. Phys. A* **34**, 7111 (2001)
[40] D Drahi, D V Sychev, K K Pirov, E A Sazhina, V A Novikov, I A Walmsley and A I Lvovsky, *Quantum* **5**, 416 (2021)
[41] A Karlsson and M Bourennane, *Phys. Rev. A* **58**, 4394 (1998)
[42] N B An, *Phys. Rev. A* **68**, 022321 (2003)
[43] D V Sychev, A E Ulanov, A A Pushkina, M W Richards, I A Fedorov and A I Lvovsky, *Nat. Photon.* **11**, 379 (2017)
[44] E V Mikheev, A S Pugin, D A Kuts, S A Podoshvedov and N B An, *Sci. Rep.* **9**, 14301 (2019)
[45] D AKuts, S A Podoshvedov and N B An, arXiv:2105.11257